Available online at www.sciencedirect.com
ScienceDirect
Applied Catalysis A: General 327 (2007) 123–131
APPLIED CATALYSIS A: GENERAL
www.elsevier.com/locate/apcata

Review

Evolution of the properties of $PtGe/Al_2O_3$ reforming catalysts with Ge content

Rafael Mariscal [a], José L.G. Fierro [a], Juan C. Yori [b], José M. Parera [b], Javier M. Grau [b,*]

[a] *Instituto de Catálisis y Petroleoquímica, CSIC C/Marie-Curie, 2, Campus de Cantoblanco, 28049 Madrid, Spain*
[b] *Instituto de Investigaciones en Catálisis y Petroquímica, INCAPE (FIQ, UNL-CONICET), Santiago del Estero 2654, S3000 AOJ Santa Fe, Argentina*

Received 1 December 2006; received in revised form 20 April 2007; accepted 1 May 2007
Available online 5 May 2007

Abstract

The effect of the Pt/Ge atomic ratio on the catalytic activity of $PtGe/Al_2O_3$ catalysts used in *n*-heptane reforming was studied. The samples were prepared by the coimpregnation method on chlorinated alumina. The platinum content was 0.5 wt.%, and Ge-loading was varied to obtain Pt/Ge atomic ratios of 0.3, 0.7, 1.4, 2.1 and 3.5. Pt/Al_2O_3 and Ge/Al_2O_3 catalysts were also prepared as references. Characterization was carried out by temperature-programmed reduction (TPR), temperature-programmed desorption of ammonia (NH_3-TPD), Fourier transform IR spectroscopy (FTIR) with CO as the probe molecule, X-ray photoelectron spectroscopy (XPS), cyclohexane (CH) dehydrogenation, and *n*-heptane reforming. The preparation method followed in this work revealed a decrease in the metallic activity of Pt due to the presence of Ge. The Ge^{2+} and Ge^{4+} species, after reduction at 500 °C, were detected on the surface of PtGe catalysts. The increase in the Ge content led to a decrease in hydrogenolysis activity and the formation of aromatics; an increase in the formation of isomers and cycloparaffins, and a reduction in the production of gas and in deactivation by coke, thereby improving catalyst stability. The results show that the maximum isoparaffin yield of all catalysts tested was obtained for a Ge-loading of 0.27 wt.% (Pt/Ge atomic ratio = 0.7). These changes in the performance of the PtGe catalysts may be attributed to the modifications occurring in the metallic and in the acid function of Pt/Al_2O_3 due to the introduction of Ge. The metallic catalytic activity of Pt is modified by the geometrical effect (dilution of Pt ensembles) and changes in the electronic properties of platinum. Ge addition produces a weakening of Pt/Al_2O_3 acid strength and an increase in the acid sites total density by the presence of Ge oxides.

Keywords: *n*-Heptane reforming; Isoparaffin selectivity; Pt/Ge atomic ratio optimization; Electronic effect

Contents

* Corresponding author. Tel.: +54 342 4533858; fax: +54 342 4531068.
E-mail address: jgrau@fiqus.unl.edu.ar (J.M. Grau).

0926-860X/$ – see front matter © 2007 Elsevier B.V. All rights reserved.
doi:10.1016/j.apcata.2007.05.007

1. Introduction

Bifunctional metal–acid catalysts were introduced into the naphtha reforming process in 1949 [1,2]. The metallic function was Pt and the acid function, chlorided Al_2O_3. During operation, this catalyst is deactivated because it is covered by the carbonaceous deposit, or coke, produced [3]. Therefore, periodic regenerations of the activity of the catalysts eliminating the coke by burning are necessary. To lengthen the operation time between regenerations, a total pressure of about 29–30 bar and a high H_2/naphtha ratio were used. The bifunctional reaction mechanisms of alkane and naphthene reactions on this catalyst were reported by Mills et al. [4]. Nearly twenty years later, the addition of a second metal, rhenium, was patented [5]. After sulphiding, this $PtRe/Al_2O_3$ catalyst produces a smaller amount of a less deactivating coke. This increases catalyst stability and allows operations to be carried out at lower pressure (about 14–17 bar). The lower hydrogen pressure produces less hydrogenolysis and a higher selectivity to aromatic hydrocarbons. $PtRe/Al_2O_3$, without sulphiding has a high hydrogenolytic activity, producing methane and other light alkanes; this disadvantage can be eliminated by sulphiding. It is considered [6] that upon sulphiding Re is covered and passivated by S and that the metallic surface consists of small ensembles of Pt atoms (1–3 atoms) diluted by inert ReS. Thus, reactions that require large ensembles of Pt atoms such as those eliciting undesirable hydrogenolysis are greatly decreased, with benefits to selectivity. Later on, other metallic promoters were incorporated to Pt. Ge [7], Sn [8] and Ir [9] were the most important. In comparison with Pt/Al_2O_3, these bimetallic catalysts have similar advantages to those of $PtRe/Al_2O_3$. In addition, $PtGe/Al_2O_3$ and $PtSn/Al_2O_3$ have the advantage over $PtRe/Al_2O_3$ and $PtIr/Al_2O_3$ of not needing sulphidation. This simplifies catalyst regeneration and allows their use in the process with continuous catalyst regeneration. Metallic Sn and Ge are not active in the reforming reactions. Only a fraction of their oxides is reduced to the metallic state and the metal interacts with or is alloyed to Pt. The inert Sn or Ge dilutes Pt atoms in the same way as Re–S in $PtRe/Al_2O_3$. Besides the geometrical or diluting Pt effect of Sn, Ge and Re–S, an electronic effect on Pt may be important [10]. The non-reduced part of the Sn, Ge and Re oxides remains on the alumina support, affecting its acid strength and changing the selectivity of the several acid-catalysed reactions.

There are several reviews covering such reforming reactions, the catalysts and the role of promoters and sulphiding. Recent reviews cover the alkane dehydrogenation mechanism for monofunctional metal catalysts [11] and the properties and characterization of the acid and metallic functions of bifunctional mono and bimetallic catalysts [12]. The latter review is a chapter of a book in the series Catalytic Naphtha Reforming [13,14], which also includes catalyst preparation, new generations of commercial catalysts, catalyst deactivation and regeneration and commercial processes.

In recent years, stringent environmental regulations have made it necessary to adjust gasoline formulations so that they will be more environmentally friendly, mainly decreasing aromatic components, which are harmful to living organisms. At the same time, it is essential to maintain naphtha quality with respect to the octane value and to decrease the number of the operative cycles by using more stable catalysts. Hence, there is an huge industrial interest in obtaining reforming catalysts able to work under processing conditions in order to increase the production of non-toxic products with high octane numbers and to prolong the useful life of the catalysts.

At present, the interest in reforming products lies in the production of isoparaffins, which have high octane numbers and low environmental pollution. It is well known that isoparaffin selectivity is controlled by the acid function, which can be altered, at the same time, achieving an improvement in stability by decreasing deactivation by coke formation. To achieve this goal, it is necessary to change the acid function, mainly its acid strength distribution, and the metallic function in order to tune the best catalyst.

Within the above framework, it seems reasonable to study the bimetallic $PtGe/Al_2O_3$ catalyst in order to see how the presence on Ge affects the metallic and the acid functions of such compounds and how this affects catalyst performance. In this system, the role of germanium as a promoter is to alter the metallic and/or acid functions. This depends on the oxidation state of the Ge promoter, which is highly dependent on the metal-loadings, the reduction temperatures, and the metal atomic ratios. These factors are important since in the reduced state Ge may be alloyed with platinum and in an oxidised form it can be stabilised by the support. Moreover, although several works have attempted to explain the promoter effect of germanium, controversy about its major role—whether this is electronic or geometric—still remains. Finally, bimetallic $PtGe/Al_2O_3$ has been less studied in the literature than the other naphtha reforming catalysts quoted above.

The present work aims at shedding light on the changes in the physicochemical and catalytic properties arising when Ge is added to Pt/Al_2O_3. The metal concentration and preparation conditions were selected appropriately according to previous experience and the Pt/Ge atomic ratio was varied to tune the catalytic activity and selectivities to comply with current requirements.

2. Experimental

2.1. Preparation of catalysts

$PtGe/\gamma\text{-}Al_2O_3\text{-}Cl$ catalysts were prepared using a standard wet impregnation technique. $\gamma\text{-}Al_2O_3$ (Cyanamid Ketjen CK300) was used as support. This material, provided in pellets, was broken, sieved between 35–80 mesh, and then calcined in air at 600 °C for 3 h. Each support was previously impregnated with a 0.2 N HCl solution (1.5 ml g^{-1} of alumina) 30 min before incorporating the metals. The precursors were added by coimpregnation with solutions of $GeCl_4$ and PtH_2Cl_6 in HCl, with a metallic concentration to obtain 0.5 wt.% of Pt and a Pt/Ge atomic ratio of 3.5, 2.1, 1.4, 0.7 and 0.3 after increasing the Ge content. In addition, monometallic Pt and Ge were prepared as references. Then, the samples were held for

24 h at room temperature. Excess solution was removed slowly by heating at a rate of 0.5 °C min^{-1} until reaching 110 °C, maintaining this temperature for 12 h. The support, impregnated and dried, was heated from room temperature to 450 °C at 3.5 °C min^{-1} in flowing air (60 ml min^{-1}), after which it was held at this temperature for 3 h. Then, flushing with N_2 over the sample for 30 min, the reduction was carried out in flowing H_2 (60 ml min^{-1}), with a programmed temperature increase of 3.5 °C min^{-1} from room temperature up to 500 °C, after which it was maintained at this temperature for 4 h. The catalyst was then cooled to room temperature in flowing hydrogen. The final catalysts were designated: Al, Pt, Ge, PtGe(*X*) (*X* = Pt/Ge atomic ratio).

2.2. Characterization techniques

Total reflection X-ray fluorescence (TXRF) analysis was employed to determine the composition of the catalysts. Measurements were performed on a Seifert EXTRA-II spectrometer (Rich Seifert & Co, Ahrensburg, Germany), equipped with an X-ray fine focus line of Mo anode, and a Si(Li) detector. Samples were ground to a powder of particle size less than 30 μm in an agate mortar and 1 ml of high-purity water was added to the powder. The sample was homogenized for 10 min by ultrasonic de-aggregation in order to disperse the possible agglomeration of particles. Two micro litres of the suspension was taken and placed on a flat plastic carrier where the water was evaporated off under vacuum.

Hydrogen adsorption isotherms were taken in order to measure the accesibility of the metal phase (Pt). First, samples were heated at 300 °C, reduced in H_2 for 1 h and degassed for 2 h. After cooling to room temperature isotherms of total and reversible hydrogen adsorption were obtained. The amount of chemisorbed hydrogen was obtained by subtracting the two isotherms and the H/Pt ratio was calculated assuming dissociative adsorption of hydrogen on the Pt atoms. A Micromeritics 2100E equipment was used for measurements.

Temperature-programmed reduction (TPR) profiles were taken on a semiautomatic Micromeritics TPD/TPR 2900 apparatus interfaced with a microcomputer. Prior to reduction, the catalysts (ca. 0.1 g loaded in a U-shaped reactor) were heated at a rate of 10 °C min^{-1} up to a final temperature of 120 °C and kept at that temperature for 1 h in a stream of helium to remove water. The samples were then cooled to room temperature under this atmosphere and switched to 5% H_2/Ar (50 ml min^{-1}) mixture. When the TCD signal of the device was constant, the TPR profile was recorded by heating the sample from room temperature to 850 °C at 10 °C min^{-1}. The effluent gas was passed through a cold trap before TCD in order to remove water from the exit stream.

Adsorption of NH_3 followed by temperature-programmed desorption was used to determine the acidity of the samples. The reduced catalysts were over reduced *in situ* at 450 °C for 30 min in a hydrogen stream. Then, they were cooled in an Ar stream to room temperature. Ammonia adsorption was studied at 25 °C with a mixture of NH_3/Ar (10% NH_3, 20 ml min^{-1}) over 15 min. Physisorbed ammonia was eliminated by flushing the sample with Ar at 80 °C for 1 h. Then, TPD was carried out in Ar flow with a heating rate of 10 °C min^{-1}. The desorbing species were detected with a quadrupole mass spectrometer (Balzers QMG).

The FTIR technique was used to study the electronic state of Pt (adsorbed CO spectra). The infrared spectra of adsorbed CO were recorded with a Nicolet 5 ZDX Fourier transform IR spectrophotometer working at a resolution of 4 cm^{-1} over the entire spectral range and averaged over 128 scans. Self-supporting wafers (ca. 10–12 mg cm^{-2}) were loaded into a sample holder, which was incorporated in an infrared cell designed to work under vacuum (a residual pressure of 10^{-4} mbar) and was fitted with greaseless stopcocks and KBr windows. The reduced catalysts were pre-reduced again *in situ* in an atmosphere of hydrogen (120 mbar) and heated at 450 °C for 1 h to remove the possible surface reoxidation of platinum in contact with the atmosphere. Following this, outgassing was carried out at the same temperature, 450 °C for 30 min. Prior to the adsorption of CO (30 mbar) at room temperature, a background spectrum of the solid was recorded. The fraction of physically adsorbed CO was removed by evacuation at room temperature for 10 min. Net infrared spectra were obtained by subtracting the sample background spectrum corresponding to CO gas and the cell windows from the whole spectrum.

X-ray photoelectron spectroscopy (XPS) experiments were accomplished with a VG Escalab 200 R spectrometer equipped with a hemispherical electron analyser and an MgK_α (1253.6 eV) X-ray source. The XPS spectrometer was equipped with a chamber for treatments under controlled gas atmospheres and allowed transfer to the analysis chamber. The reduced catalysts were pre-reduced under treatment with hydrogen *in situ* at 450 °C for 1 h. After outgassing at 10^{-5} mbar, the samples were transferred to the ion-pumped analysis chamber, whose residual pressure was kept below 7×10^{-9} mbar during data acquisition. Binding energies (BE) were referenced to the Al 2p peak (74.5 eV) as an internal standard to take into account the effect of charge. The accuracy of the BE was ± 0.1 eV. Al 2p, Pt 4d, Ge 2p, Cl 2p and O 1s regions of the XPS spectrum were scanned a number of times in order to obtain a good signal-to-noise ratio. Peak intensities were estimated by calculating the integral of each peak after subtracting an S-shaped background and fitting the experimental peak to a combination of Lorentzian/Gaussian lines of variable proportions. Surface atom ratios were calculated from peak area ratios normalized by using the corresponding atomic sensitivity factors [15].

2.3. Activity measurements

The catalyst was charged in a glass tubular fixed-bed reactor of 8 mm internal diameter, forming a cylindrical bed of 6 mm of height, and was reduced *in situ* with hydrogen (60 ml min^{-1}) for 2 h at 450 °C before each reaction test to remove the possible surface reoxidation of platinum in contact with atmosphere. Cyclohexane (Merck 99.9%) dehydrogenation was performed at 300 °C, 1 bar, catalyst mass = 0.1 g, WHSV = 10 h^{-1} and molar ratio H_2/C_6H_{12} = 30. The reaction

products were analysed by on-line chromatography using a packed column (1/8″ O.D., 2 m) with FFAP on Chromosorb P. In the reforming of *n*-heptane (Carlo Erba RPA) 0.15 g of catalyst was used. The reaction conditions were 450 °C, 1 bar, WHSV = 3.4 h^{-1} and molar ratio $H_2/n\text{-}C_7 = 7.3$. Maximum time-on-stream was 6 h. $n\text{-}C_7$ conversion, selectivities and yields to the different products (on a carbon basis) were calculated from the chromatographic data. Selectivity was calculated according to the following formula:

$$\mathrm{Si} = \frac{A_i \mathrm{rf}_i \mathrm{CN}_i 100}{X \sum A_i r f_i \mathrm{CN}_i} \quad (1)$$

where: X is the total conversion, A_i is the chromatographic area of the ith compound, rf_i is the response factor of the ith compound, and CN_i is the carbon number of the ith compound. The yield is calculated by multiplying the selectivity by the conversion.

3. Results and discussion

3.1. Catalyst characterization

The metal and chloride contents and the properties of metallic function, H/Pt and activity of the Pt, Ge, and PtGe catalysts are given in Table 1. Chemical analysis, determined by the TXRF technique, revealed that the experimental metallic concentrations of the samples were similar to the theoretical ones. The hydrogen chemisorption capacity decreases when Ge is added to the catalyst. Regarding metallic function activity, evaluated by cyclohexane (CH) conversion to benzene after 2 h on-stream and expressed by the turnover frecuency (TOF) (CH converted molecules/exposed Pt atom x seconds), monometallic Pt was the most active catalyst, producing a TOF = 1.8. For PtGe bimetallic catalysts, Table 1 shows a drop in the TOF values from 1.7 to 1.3, occurred with an increase in the germanium content (in the range of 0.05–0.27%). For higher Ge content, 0.62%, the drop is higher, TOF = 0.3. This reaction is structure-insensitive in the sense of Boudart [16] and hence should not depend on Pt crystal size and geometry, being proportional only to the exposed metallic surface. The results of hydrogen chemisorption and cyclohexane dehydrogenation suggest a decrease in the exposed metallic area. This reduction may be due to the covering of platinum atoms by the germanium promoter or alloyed PtGe clusters formation [17]. Alternatively, it could also be ascribed to metal-promoter and metal-support effects according to Douidah et al. [18]. This possibility is supported by the TPR diagrams, discussed later, which show hindrance in the reduction of Pt oxide. This delay in the two TPR peaks when Ge is present ranges from 225 to 240 °C and from 360 to 380 °C. At higher temperatures it would be considered that all Pt is in the metallic state and that it catalyses the reduction of Ge oxides. Besides the covering of some Pt atoms by Ge, which dilutes the rest of the active Pt atoms (geometrical effect), the decrease in metallic activity could also be ascribed to the electronic effect on Pt produced by the presence of germanium oxide, as shown later by FTIR. Pt transfers some electronic density to GeO_x and the electron-deficient Pt atom ($Pt^{\delta+}$) has a weaker adsorption capacity of CH than metallic Pt atom (Pt^0), accounting for the decrease in metallic catalytic activity. Additional evidence that the formation of PtGe clusters increases the electrophilic character of Pt was obtained from the results of IR spectroscopy using CO as probe molecule and the competitive hydrogenation reaction of mix of benzene and toluene by Borgna et al. [17].

Table 1
Chemical composition, H_2 chemisorption capacity and activity of the metallic function of Pt, Ge, and PtGe catalysts evaluated by cyclohexane (CH) conversion to benzene attained at 2 h

Catalyst	% wt. Pt	% wt. Ge	% wt. Cl	H/Pt (%)	TOF[a]
Pt	0.50	–	0.91	54	1.8
PtGe(3.5)	0.51	0.05	0.88	52	1.7
PtGe(2.1)	0.48	0.09	0.91	48	1.4
PtGe(1.4)	0.51	0.13	0.92	38	1.3
PtGe(0.7)	0.48	0.27	0.90	31	1.3
PtGe(0.3)	0.49	0.62	0.89	11	0.3
Ge	–	0.51	0.89	–	–

[a] (CH converted molecules/exposed Pt atom x seconds).

The TPR profiles of the calcined monometallic (Pt and Ge) and bimetallic PtGe samples are shown in Fig. 1. In order to further clarify the discussion the peaks have been deconvoluted. The TPR profile of the monometallic Pt catalyst displays a major peak with a maximum at 225 °C (peak I), attributed to the reduction of oxychlorided platinum species on the surface and a little shoulder at ca. 360 °C (peak II) associated with the reduction of platinum species interacting strongly with the support [19,20]. The monometallic Ge sample displays a single reduction peak with a maximum at 620 °C (peak III), which can be attributed to Ge^{4+} reduction [20]. The TPR profiles of the

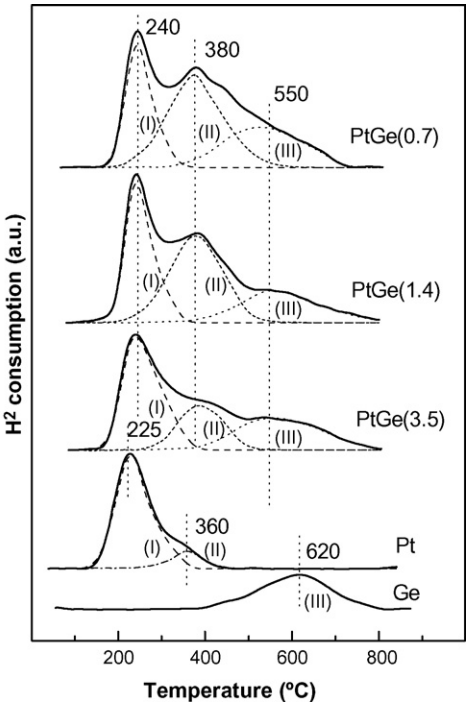

Fig. 1. TPR profiles of calcined Pt, Ge and PtGe/Al_2O_3 catalysts.

bimetallic PtGe catalysts exhibited three peaks at 240, 380 and 550 °C. On comparing these profiles with that of monometallic catalyst, it may be seen that the germanium interacting with platinum delays the reduction of the platinum oxides. The peaks at 225 and 360 °C on Pt are retarded at 240 and 380 °C, respectively, on PtGe. At the same time, the platinum promotes the reduction of Ge^{4+} ions at lower temperatures [21]. In addition, with increasing germanium loading the intensity of the peak I decrease and the shoulder at 380 °C (peak II) increases. Thus, the TPR profiles of the bimetallic PtGe catalysts show an important interaction between platinum and germanium species occurs in all bimetallic samples. The possibility of PtGe alloying cannot be neglected. Previous works addressing the state of the surface species on the PtGe/Al_2O_3 catalyst revealed that on samples reduced at temperatures as high as 650 °C [20–23] germanium is present as Ge^{2+} and Ge^0, the latter being alloyed with Pt. Some of the differences with the literature cited above can be explained by considering differences in the metal precursors and preparation methods that influence the metallic clusters [24].

The chemisorption of CO was used to reveal the nature of the metal surface sites in the reduced catalysts. The IR spectra of CO chemisorbed on the Pt, Ge, and PtGe catalysts are shown in Fig. 2. The infrared spectrum of CO adsorbed on the Pt catalyst displays an absorption band at 2070 cm^{-1}, corresponding to linearly adsorbed CO on metallic platinum [25]. In contrast to the Pt catalyst, the Ge sample does not show any absorption band. The TPR diagram of the Ge/Al_2O_3 catalyst (see Fig. 1) shows some initial reduction at 500 °C, the reduction temperature during catalyst preparation. The FTIR diagram of this catalyst shows no adsorption of CO. The same result was found upon reducing the catalyst at 700 °C, and hence the absorption bands observed in the bimetallic samples can only be attributed to the CO adsorbed on the platinum species and not to the CO adsorbed on the Ge or partially reduced GeO_x. As shown in Fig. 2, when the Pt/Ge atomic ratio decreased, the germanium content increased and the absorption band maximum was shifted to higher wavenumbers: 2083 cm^{-1}. This upward shift occurs in the opposite direction to that expected, if a simple diluting effect of the Ge atoms in the CO layer occurs. Thus, this observation could be associated with Ge atoms acting as electron-acceptor sites [17,26], decreasing the electronic density of platinum. As a consequence, the back-donation of electrons from the Pt atoms to the empty antibonding π^* orbital of chemisorbed CO is less intense. Moreover, even a shoulder at 2120 cm^{-1} appears clearly for the sample with the highest germanium concentration, which is assigned to CO bonded on $Pt^{\delta+}$ [27,28]. These observations suggest that the germanium promoter is able to remove electronic density from platinum atoms, generating a charged electron-deficient atom that weakens the adsorption capacity of surface platinum atoms. This explanation agrees with the decline in metallic activity tested by cyclohexane dehydrogenation, see Table 1.

FTIR with CO adsorption is a technique that exclusively probes the surface sites. As a consequence, it can be said that on the catalyst surface exist only Pt^0 and $Pt^{\delta+}$ species. The presence of oxidized platinum species in the surface would imply appearance of new absorption bands in the range of 2130–2150 cm^{-1} [27,29,30].

NH_3 TPD spectra are shown in Fig. 3 for the support, Al, and the catalysts Pt and PtGe(0.7). All samples shows a similar spectrum, characterized by two desorption peaks centred at 326 and 650 °C. The first one can be attributed to ammonia

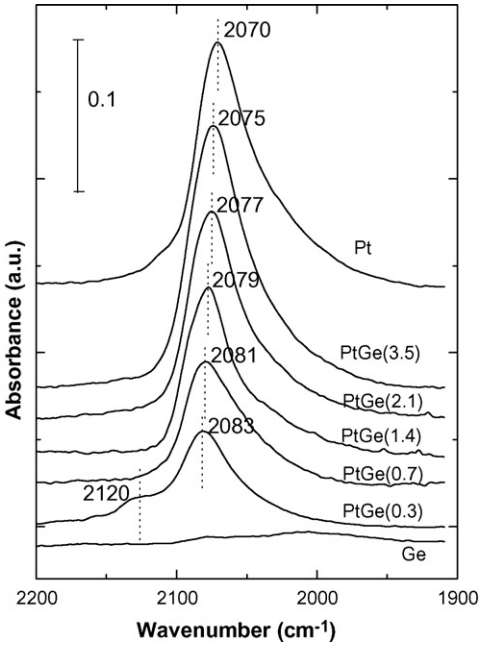

Fig. 2. FTIR spectra of Pt, Ge and PtGe/Al_2O_3 reduced catalysts after CO adsorption and outgassing at room temperature.

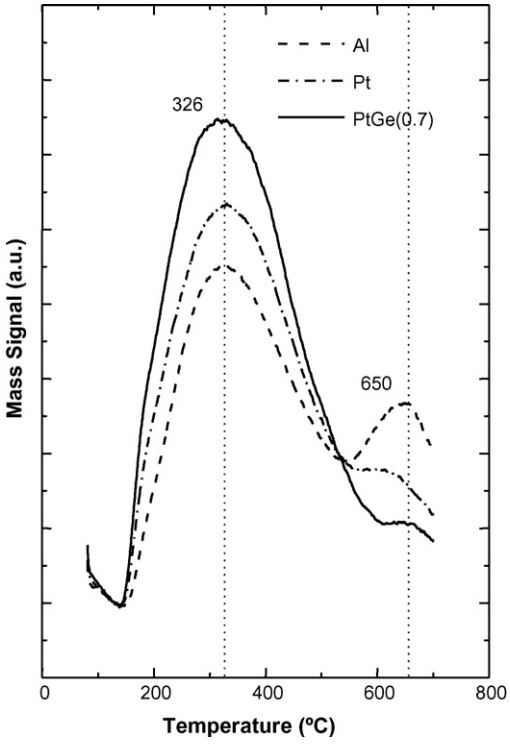

Fig. 3. TPD profiles of reduced Pt, Ge and PtGe/Al_2O_3 catalysts.

Table 2
Binding energies (eV) of core electrons of reduced Pt, Ge, and PtGe catalysts

Catalyst	Al 2p	Pt $4d_{5/2}$	Ge $2p_{3/2}$	Cl $2p_{3/2}$
Pt	74.5	314.9	–	198.9
PtGe(3.5)	74.5	315.0 (62)	1220.1	198.9
		317.9 (38)		
PtGe(2.1)	74.5	315.0 (61)	1220.0	198.8
		317.9 (39)		
PtGe(1.4)	74.5	315.0 (52)	1219.9	198.8
		317.9 (48)		
PtGe(0.7)	74.5	315.0 (40)	1219.9	198.8
		317.9 (60)		
PtGe(0.3)	74.5	315.0 (39)	1220.0	198.8
		317.9 (61)		
Ge	74.5	–	1220.1	198.8

adsorbed to weak and mild acid sites. The second one corresponds to ammonia adsorbed to strong acid sites. The addition of Pt to Al_2O_3 elicits a decrease in the peak at 650 °C and an increase in the peak at 326 °C. When Ge was added to the Pt/Al_2O_3 catalyst, the peak at 326 °C increases further and the peak at 650 °C almost completely disappeared. It may therefore be concluded that the addition of Ge produces a weakening of the Pt/Al_2O_3 acid strength and an increase in the acid site total density.

To shed further light on the above, the chemical state of the catalyst metallic components and the relative concentrations at the surface were evaluated by XPS in H_2-reduced samples. The energy regions of the Al 2p, Pt $4d_{5/2}$, Ge $2p_{3/2}$ and Cl 2p core levels were scanned. Although the most intense photoemissions lines of platinum were those arising from Pt 4f core levels, this energy region became overshadowed by the presence of a very strong Al 2p peak. Consequently, the energy region of the less intense Pt 4d peak was scanned for all the Pt-containing samples. The binding energies (BE) of the core electrons of the most abundant elements of the reduced PtGe/Al_2O_3 catalysts are summarized in Table 2. For the reduced Pt monometallic catalyst, the binding energy of the Pt $4d_{5/2}$ level appeared at 314.9 eV, which can be assigned to Pt^0 [22,23,31,32]. For PtGe bimetallic samples, the BE of the Pt $4d_{5/2}$ peak suggests the possible presence of more than one platinum species (full-width at half-maximum values, higher than 2.0 eV in all cases), and this peak can be deconvoluted into two contributions at 315.0 and 317.9 eV, the latter indicating a change in oxidation state and more specifically it was associated to Pt^{2+} ions by the presence of oxide-like species of platinum on the catalyst surfaces [33]. The percentages of these peaks are shown in brackets in Table 2. In general, an increase in oxidized Pt with the Ge content was observed. The apparent inconsistency between the results obtained from both characterization techniques may be explained with the following reasoning: it is known that the penetration depth of XPS is between 2 and 5 nm, which is more than one layer and therefore it is not a measurement limited to the superficially exposed atoms. By the contrary FTIR with CO adsorption is a technique that exclusively probes the surface sites.

As mentioned above, an important issue in these bimetallic catalysts is the oxidation state of the germanium species. It is clear that the state of the promoter in these catalysts is strongly dependent on metal loadings and reduction temperatures. Ge $2p_{3/2}$ binding energy is essentially analogous for all catalysts, see Table 2. It appeared ca. 1220.0 eV, and this peak is attributed to Ge^{2+}/Ge^{4+} [32]. The Binding energy for Al 2p at 74.5 eV was taken as a reference and, finally, chloride ion was detected at the surface of all samples, with a BE of the Cl $2p_{3/2}$ peak at ca. 198.8 eV [32,34]. It should be noted that no Ge^0 was found on the surface of catalysts reduced at 500 °C, in agreement with previous work [31,35,36]. These observations do not contradict other reports from the literature, in which alloys were detected between platinum and germanium and have been reported in this kind of catalyst previously [22], because these alloys were reported for higher Pt-loadings and/or higher reduction temperature than the one used in the present work. Additionally, the positive role of alloy formation in catalyst performance has been seriously questioned because Pt–Ge alloys are inactive [37].

Table 3 lists the surface atomic ratios derived from the XPS measurements. The Pt/Al atomic ratios increased from 1.4×10^{-3} to 7.9×10^{-3} in the range of Ge variation. A very small part of that increase may be due to the decrease in the surface Al atom concentration due to coverage with Ge. This increase is very small because the Ge atomic concentration is three orders of magnitude lower than the surface Al atomic concentration (Table 3). Thus, the fraction of Al coverage by Ge is very small, influencing the Pt/Al atomic ratio very little. This suggests that the external surface of the catalyst particles becomes Pt-enriched or that Pt dispersion is increased. An increase of metallic dispersion would be concordant with an increase of the metallic activity in the CH dehydrogenation reaction. Nevertheless, we have observed that when increase of the Ge-loaded, the metallic activity drop off (to see Table 1). An explanation of this fact can be given if it is considered that the amount of electron-deficient Pt atom ($Pt^{\delta+}$) increases with the Ge content and that these atoms are less efficient in the CH deshydrogenation that the metallic particles of Pt^0. Hydrogen chemisorption results (Table 1) showed that Pt dispersion decreases upon Ge incorporation. Similar results were reported by de Miguel et al. [21], whereas Goldwasser et al [23] pointed out that GeO_x species can be stabilized on the alumina surface, while dilution or geometric effects would be precluded under the experimental conditions employed. In contrast, Huang et al. [36] showed that a highly dispersed Pt sample was not affected by the incorporation of germanium. The surface concentration

Table 3
Surface atomic ratios of Pt, Ge, and PtGe reduced catalysts according to XPS data

Catalyst	Pt/Al at $\times 10^3$	Ge/Al at $\times 10^3$	Pt/Ge at	Cl/Al at $\times 10^2$
Pt	0.8	–	–	3.1
PtGe(3.5)	1.4	1.0	1.41	1.8
PtGe(2.1)	1.6	1.3	1.25	1.6
PtGe(1.4)	2.5	1.9	1.30	1.6
PtGe(0.7)	3.9	5.3	0.73	1.7
PtGe(0.3)	7.9	13.6	0.58	1.5
Ge	–	6.0	–	1.4

of germanium increases more dramatically than that of platinum with the germanium content, and hence the surface atomic ratio Pt/Ge clearly falls. In Table 3, the surface Cl/Al atomic ratios are similar for all bimetallic samples, some being higher for the platinum monometallic catalyst. This means that Cl, and possibly surface acidity, are nearly proportional to surface Al not covered by Ge and Pt.

In sum, the effects on the physicochemical properties of Pt/Al_2O_3 caused by germanium incorporation are as follows: (i) an important interaction is seen between metallic Pt ensembles and Ge^{4+}/Ge^{2+} ions stabilized by the alumina support in these bimetallic catalysts (changes in the TPR and XPS analysis); (ii) germanium acts as an electron-acceptor element, decreasing the electronic density of platinum (electronic effect), as evidenced by FTIR; (iii) Ge oxides interact with the stronger acid sites of the support, weakening its acid strength and increasing the total acidity, as evidenced by NH_3-TPD.

3.2. Evaluation of n-heptane reforming catalysts

Fig. 4 shows the evolution of *n*-heptane conversion as a function of the germanium content in the PtGe/Al_2O_3 catalysts for different reaction times (5, 30, 60 and 120 min). Both the activity and stability of the catalysts changed with the incorporation of the Ge promoter. At low Ge-loadings, conversion was higher than for the Pt monometallic catalyst until an activity maximum was reached; this took place in the PtGe(0.7) catalyst, whose Ge-loading was 0.27 wt.%. For the PtGe(0.3) catalyst, with a higher Ge-content, activity decreased dramatically. Another beneficial effect of the introduction of Ge was an improvement in catalyst stability. This was verified by comparing the drop in conversion with the reaction time for the Pt monometallic catalyst with that of the PtGe bimetallic catalysts, mainly between fresh catalysts (5 min) and the pseudo-stationary state (30 min).

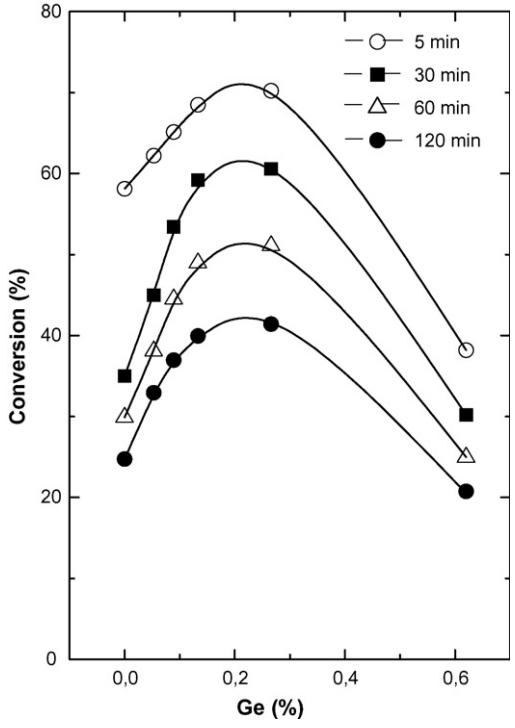

Fig. 4. Total conversion of *n*-heptane as a function of Ge content (expressed wt.%) for PtGe/Al_2O_3 catalysts at different times of the reforming reaction.

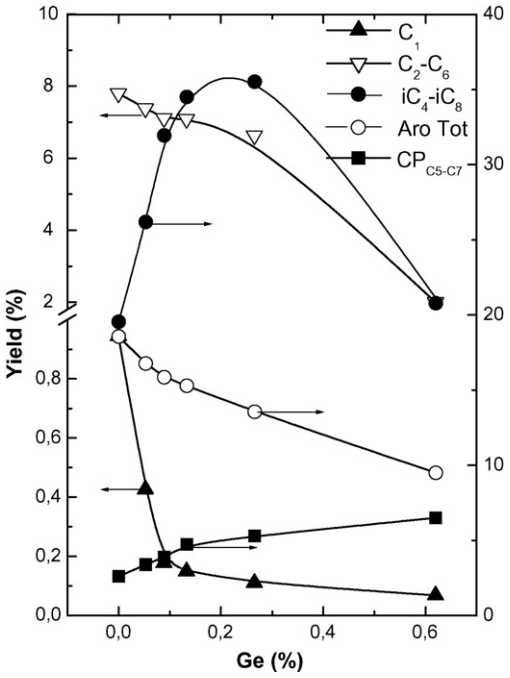

Fig. 5. Product yield as a function of the Ge content (expressed wt.%) for PtGe/Al_2O_3 catalysts at time = 5 min.

Fig. 5 shows the yield to different products as a function of the Ge-loading. The yield values shown were selected after 5 min of on-stream operation. The products of *n*-heptane reforming were arranged according to the literature [4,13] as follows: methane (C_1), as a pattern of the capacity of hydrogenolysis of the metallic function; normal paraffins (C_2–C_6), to evaluate the cracking activity for gas production of the acid function; isoparaffins from C_4 to C_8 (*i*-C_4–*i*-C_8), to determine changes in the formation of isomers on the acid function; cycloparaffins from C_5 to C_7 ($CP_{C5–C7}$), produced by the bifunctional metal–acid mechanism, and total aromatics (Bz + Tol), to determine the dehydrocyclization capacity (Aro Tot) produced by the bifunctional mechanism. Upon relating the selectivity changes caused by the incorporation of Ge, it may be observed that the evolution of yield underwent a strong increase in the direction of the formation of isoparaffins, a maximum being reached for a Ge-loading of 0.27 wt.%. In addition, the increase in the Ge-content was accompanied by an increase in cycloparaffin formation, whereas total aromatics followed the opposite trend; cracking products and hydrogenolysis products were observed and decreased with the Ge content.

Cracking and isomerization are reactions controlled by the acid function of the catalyst. The first requires strong acid sites and the second mild acid strength. The decrease in cracking (C_2–C_6) and the increase in isomerization (*i*-C_4–*i*-C_8) caused by the addition of Ge to Pt/Al_2O_3 is due to the weakening of the acid strength of the sites, as shown before. Strong acidity

Table 4
n-heptane reaction on monometallic, PtGe and PtRe bimetallic catalysts

	Catalysts						
	Pt	PtGe(3.5)	PtGe(2.1)	PtGe(1.4)	PtGe(0.7)	PtGe(0.3)	PtRe(1.0)*
Ge, wt.%	–	0.05	0.09	0.13	0.27	0.62	0.30
X_f	24.7	32.9	36.9	39.9	41.4	19.8	28.4
$(X_i - X_f)/X_i$	0.57	0.47	0.43	0.42	0.41	0.52	0.57
Y C_1	0.27	0.16	0.11	0.12	0.08	0.04	0.23
Y bz	0.32	0.13	0.15	0.16	0.17	0.10	0.28
Y tol	3.29	7.27	7.01	7.02	5.09	1.66	4.03
Y i-C_{4-8}	13.46	17.11	20.74	22.86	24.47	13.38	12.67
i-C_{4-8}/Aro_{tot}	3.54	2.31	2.90	3.17	4.65	7.60	3.14

(*): from previous work ref. [40], X_i: conversion of *n*-heptane at 5 min time-on-stream, X_f: conversion of *n*-heptane at 120 min time-on-stream, Y: yield of each product at 120 min time-on-stream, C_1: methane, bz: benzene, tol: toluene, i-C_7: heptane isomers

decreases and total acidity increases with the increase in Ge. For a large excess of Ge (0.62%), the metallic sites begin to decrease their dehydrogenating activity, as can be seen in Table 1 (dehydrogenation of cyclohexane), due to electronic effects, and the selectivity of isomerization also declines. This beneficial effect on selectivity produced by the weakening of acidity by the addition of Ge is similar to that produced by the addition of Sn to a PtRe catalyst [38].

Since PtRe/Al_2O_3 is a catalyst widely used in commercial naphtha reforming, its catalytic behaviour in *n*-heptane reforming was compared with that of the Pt catalyst and with those of the bimetallic series of PtGe. For the monometallic Pt, the PtGe bimetallics and the commercial type PtRe (1.0) with 0.3% Pt and 0.3% Re, Table 4 shows the conversion, stability (difference in conversion from the beginning to the end of the run), and yield to several products. The advantage of PtGe (0.7) with 0.27% Ge is clear. This catalyst has the highest values of conversion, stability (lowest drop in conversion), yield to isomers and the lowest value of C_1 (hydrogenolysis) and toluene and has the most favourable isomers/aromatics ratio. Under these conditions, PtGe (0.3) was not considered because shows very low activity.

The physicochemical and catalytic properties of Pt monometallic catalysts were modified in the bimetallic catalysts by change in the Pt/promoter atomic ratio. The incorporation of germanium decreased the dehydrogenating capacity of platinum and much more so the reaction rate of structure-sensitive reactions, such as hydrogenolysis. This may be due to a geometric effect: destruction of the large ensembles of Pt atoms necessary for hydrogenolysis produced by dilution of surface Pt atoms with inert Ge atoms. It may also be due to an electronic effect, with charge transference from the Pt to the promoter. Both effects of Ge on Pt act simultaneously. A clear difference in the action of Ge in a non-demanding reaction (the dehydrogenation of cyclohexane, Table 1) and a demanding reaction (C_1 produced by hydrogenolysis, Fig. 5 and Table 4) can be seen on comparing monometallic Pt with bimetallic PtGe with 0.09% Ge. CH conversion on Pt present a drop in TOF value from 1.8 to 1.4 upon the addition of Ge (it fell 1.3 times) while the C_1 yield fell from 0.27 to 0.11 (2.5 times). The reactions catalysed by the acid function, hydrocracking and isomerization, show a behaviour that can be explained in terms of the changes in the acid strength of the support sites (Fig. 3). When the Ge content is increased, the strength of the acid sites decreases, decreasing hydrocracking, which requires strong acidity, and increasing isomerization, which requires intermediate acidity (Fig. 5). There was an optimised ratio for a germanium content of 0.27 wt.%, corresponding to the PtGe bimetallic catalyst (0.7). The catalyst with the highest Ge-content (0.62%) showed a strong inhibition of catalytic activity. Thus, it appears possible to control the distribution of reforming products by tuning the Ge-content in bimetallic PtGe catalysts [39], thereby opening a way to improve the environmental quality of the gasoline pool without altering its specifications as regards the octane value. Accordingly, the decline in aromatics can be replaced by an increase in naphthene and isoparaffin products.

4. Conclusions

Study of the surface and catalytic properties of PtGe/Al_2O_3 bimetallic catalysts has shown that, compared to Pt, the platinum and germanium coimpregnation procedure produces an increase in isoparaffin and cycloparaffin production in the reforming of linear hydrocarbon fractions. An increase in the liquid fraction and an improvement in catalytic stability were also obtained. In contrast, a decrease in the formation of aromatics was observed. Reforming fractions with PtGe/Al_2O_3 bimetallic catalysts is more appropriate than with Pt monometallic catalysts and PtRe catalyst to comply with current environmental specifications, maintaining quality regarding octane numbers. The bimetallic catalyst with a germanium content of 0.27 wt.% showed maximum activity and isoparaffin selectivity.

Acknowledgement

This work was supported by Project N° 2002AR0010 and within the Frame Programme of Cooperation between Spain (CSIC) and Argentina (CONICET).

References

[1] V. Haensel, US Patent 2,479,109 (1949), to UOP.
[2] V. Haensel, US Patent 2,479,110 (1949), to UOP.

[3] J.P. Frank, G. Martino, in: J.L. Figueiredo (Ed.), Progress in Catalyst Deactivation, Martinus Nijhoff Publ, The Hague, 1982, 355.
[4] G.A. Mills, H. Heinemann, T.H. Milliken, A.G. Oblad, Ind. Eng. Chem. 45 (1953) 134.
[5] H. E. Kluksdahl, U.S. Pat. 3,415,737 (1968) to Chevron Res. Co.
[6] B. Biloen, J.H. Helle, H. Verbsbeck, F.M. Dautzenberg, W.H.M. Sachtler, J. Catal. 63 (1980) 112.
[7] K. R. McCallister, T. P. O'Neal, French Patent 2,078,056 (1971), to UOP.
[8] R. E. Rausch, U.S. Pat. 3,745,112 (1975), to UOP.
[9] J. H. Sinfelt, U.S. Pat. 3,953,368 (1976), to Exxon.
[10] L. S. Carvalho, C. L. Pieck, M. C. Rangel, N. S. Fígoli, J. M. Grau, P. Reyes, J. M. Parera, Appl. Catal. A 269 (2004) 91.
[11] B.H. Davis, Catal. Today 53 (1999) 443.
[12] B.H. Davis, G.J. Antos, in: G.J. Antos, A.M. Aitani (Eds.), Catalytic Naphtha Reforming, second ed., Marcel Dekker, Inc, New York, 2004, p. 199.
[13] G.J. Antos, A.M. Aitani, J.M. Parera (Eds.), Catalytic Naphtha Reforming Science and Technology, Marcel Dekker, Inc, New York, 1995.
[14] G.J. Antos, A.M. Aitani (Eds.), Catalytic Naphtha Reforming Revised and Expanded, second ed., Marcel Dekker, Inc., New York, 2004.
[15] C.D. Wagner, L.E. Davis, M.V. Zeller, J.A. Taylor, R.H. Raymond, L.H. Gale, Surf. Interface Anal. 3 (5) (1981) 211.
[16] M. Boudart, A. Aldag, J.E. Benson, N.A. Dougharty, C.G. Harkins, J. Catal. 6 (1966) 92.
[17] A. Borgna, T.F. Garetto, C.R. Apesteguia, B. Moraweck, Appl. Catal., A 182 (1999) 189.
[18] A. Douidah, P. Marécot, S. Szabo, J Barbier, Appl. Catal., A 225 (2002) 21.
[19] H. Lieske, G. Lietz, H. Spindler, J Volter, J. Catal. 81 (1983) 8.
[20] S.R. de Miguel, O.A. Scelza, A.A. Castro, Appl., Catal. 44 (1988) 23.
[21] S.R. de Miguel, J.A. Martinez Correa, G.T. Baronetti, A.A. Castro, O.A. Scelza, Appl. Catal. 60 (1990) 47.
[22] R. Bouwman, P. Biloen, J. Catal. 48 (1977) 209.
[23] J. Goldwasser, B. Arenas, C. Bolivar, G. Castro, A. Rodriguez, A. Fleitas, J. Giron, J. Catal. 100 (1986) 75.
[24] J.H. Sinfelt, Bimetallic Catalysts, John Willey & Sons, New York, 1983
[25] M.G.V. Mordente, C.H. Rochester, J. Chem. Soc. Far. Trans. I 85 (1989) 3495.
[26] T. Romero, B. Arenas, E. Perozo, C. Bolivar, G. Bravo, P. Marcano, C. Scott, M.J. Pérez Zurita, J. Goldwasser, J. Catal. 124 (1990) 281.
[27] A.V. Ivanov, L.M. Kustov, Russ. Chem. Bull. 47 (1998) 1061.
[28] A.V. Ivanov, A. Yu Stakheev, L.M. Kustov, Russ Chem. Bull. 48 (1999) 1255.
[29] C. Morterra, G. Cerrato, S. Di Ciero, M. Signoretto, F. Pinna, G. Strukul, J. Catal. 165 (1997) 172.
[30] A.V. Ivanov, L.M. Kustov, T.V. Vasina, V.B. Kazanskii, P. Zeuthen, Kinet. Catal. 38 (1997) 403.
[31] C. Larese, J.M. Campos-Martin, J.L.G. Fierro, Langmuir 16 (2000) 10294.
[32] D. Briggs, M.P. Seah, Practical Surface Analysis, second Ed., John Willey & Sons, 1993.
[33] B. Grbic, N. Radic, B. Markovic, P. Stefanov, D. Stoychev, Ts. Marinova, Appl. Catal., B 64 (2006) 51.
[34] D. Briggs, M.P. Seah (Eds.), Practical Surface Analysis, second ed., Auger and X-ray Photoelectron Spectroscopy, vol. 1, Wiley, Chichester, 1990.
[35] G.J. Arteaga, J.A. Anderson, C.H. Rochester, J. Catal. 189 (1999) 195.
[36] Z. Huang, J.R. Fryer, C. Park, D. Stirling, G. Webb, J. Catal. 175 (1998) 226.
[37] N. Macleod, J.R. Fryer, D. Stirling, G. Webb, Catal. Today 46 (1998) 37.
[38] V.A. Mazzieri, J.M. Grau, C.R. Vera, J.C. Yori, J.M. Parera, C.L. Pieck, Catal. Today 107–108 (2005) 643.
[39] A. Wootsch, L. Pirault-Roy, J. Leverd, M. Guérin, Z. Paál, J. Catal. 208 (2002) 490.
[40] V.A. Mazzieri, J.M. Grau, C.R. Vera, J.C. Yori, J.M. Parera, C.L. Pieck, Appl. Catal., A 296 (2005) 216–221.